



Network-Based Approach and IVI Methodologies, a Combined Data Investigation Identified Probable Key Genes in Cardiovascular Disease and Chronic Kidney Disease

Mohd Murshad Ahmed¹, Safia Tazyeen¹, Shafiu Haque², Ahmad Sulimani³, Rafat Ali⁴, Mohd Sajad¹, Aftab Alam¹, Shahnawaz Ali⁵, Hala Abubaker Bagabir⁶, Rania Abubaker Bagabir⁷ and Romana Ishrat^{1*}

OPEN ACCESS

Edited by:

Christoph D. Rau,
University of North Carolina at Chapel
Hill, United States

Reviewed by:

Mohd Amir,
Jamia Millia Islamia, India
Shahzaib Ahmad,
International Centre for Genetic
Engineering and Biotechnology, India

*Correspondence:

Romana Ishrat
rishrat@jmi.ac.in
orcid.org/0000-0001-9744-9047

Specialty section:

This article was submitted to
Cardiovascular Genetics and Systems
Medicine,
a section of the journal
Frontiers in Cardiovascular Medicine

Received: 08 August 2021

Accepted: 17 November 2021

Published: 05 January 2022

Citation:

Ahmed MM, Tazyeen S, Haque S,
Sulimani A, Ali R, Sajad M, Alam A,
Ali S, Bagabir HA, Bagabir RA and
Ishrat R (2022) Network-Based
Approach and IVI Methodologies, a
Combined Data Investigation Identified
Probable Key Genes in Cardiovascular
Disease and Chronic Kidney Disease.
Front. Cardiovasc. Med. 8:755321.
doi: 10.3389/fcvm.2021.755321

¹ Centre for Interdisciplinary Research in Basic Sciences, Jamia Millia Islamia, New Delhi, India, ² Research and Scientific Unit, College of Nursing and Allied Health Science, Jazan University, Jazan, Saudi Arabia, ³ Department of Medical Laboratory Technology, College of Applied Medical Sciences, Jazan University, Jazan, Saudi Arabia, ⁴ Department of Bioscience, Jamia Millia Islamia, New Delhi, India, ⁵ Centre for Stem Cell & Regenerative Medicine, KING' College London, Guy's Hospital, London, United Kingdom, ⁶ Department of Medical Physiology, Faculty of Medicine, King Abdulaziz University, Rabigh, Saudi Arabia, ⁷ Department of Hematology and Immunology, College of Medicine, Umm-Al-Qura University, Mecca, Saudi Arabia

In fact, the risk of dying from CVD is significant when compared to the risk of developing end-stage renal disease (ESRD). Moreover, patients with severe CKD are often excluded from randomized controlled trials, making evidence-based therapy of comorbidities like CVD complicated. Thus, the goal of this study was to use an integrated bioinformatics approach to not only uncover Differentially Expressed Genes (DEGs), their associated functions, and pathways but also give a glimpse of how these two conditions are related at the molecular level. We started with GEO2R/R program (version 3.6.3, 64 bit) to get DEGs by comparing gene expression microarray data from CVD and CKD. Thereafter, the online STRING version 11.1 program was used to look for any correlations between all these common and/or overlapping DEGs, and the results were visualized using Cytoscape (version 3.8.0). Further, we used MCODE, a cytoscape plugin, and identified a total of 15 modules/clusters of the primary network. Interestingly, 10 of these modules contained our genes of interest (key genes). Out of these 10 modules that consist of 19 key genes (11 downregulated and 8 up-regulated), Module 1 (RPL13, RPLP0, RPS24, and RPS2) and module 5 (MYC, COX7B, and SOCS3) had the highest number of these genes. Then we used ClueGO to add a layer of GO terms with pathways to get a functionally ordered network. Finally, to identify the most influential nodes, we employed a novel technique called Integrated Value of Influence (IVI) by combining the network's most critical topological attributes. This method suggests that the nodes with many connections (calculated by hubness score) and high spreading potential (the spreader nodes are intended to have the most impact on the information flow in the network) are

the most influential or essential nodes in a network. Thus, based on IVI values, hubness score, and spreading score, top 20 nodes were extracted, in which RPS27A non-seed gene and RPS2, a seed gene, came out to be the important node in the network.

Keywords: CVD, CKD, PPIN network, IVI, hubness score, spreading score

INTRODUCTION

The risk of getting cardiovascular disease (CVD) in patients with chronic kidney disease (CKD) is more than without CKD as discussed by Jankowski et al. (1). Chronic kidney disease (CKD) is a systemic condition that affects almost 10% of the population. The prevalence of CKD has increased in recent decades due to aging which affects about one out of every 10 people (2). Multiple studies have confirmed that individuals with renal disease undergo rapid aging, which accelerates the onset of pathologies, such as CVD, which is strongly correlated with older age. Furthermore, patients with CKD are more prone to CVD and even death due to the progression of end-stage renal disease (ESRD) (3). CVD, along with chronic renal disease, remains the leading cause of morbidity and mortality in individuals, particularly in those involving a systemic inflammatory process, such as atherosclerosis (4). CKD is the 14th leading cause of mortality, with the death rate anticipated to increase to 14 per 100,000 people by 2030 (5). Despite the rising pervasiveness of CKD and its frequent combination with CVD, patients with severe CKD (eGFR 30 ml/min per 1.73 m²) were commonly omitted from key randomized controlled studies (6). Traditional CVD risk factors, such as hypertension, advanced age, diabetes, male sex, dyslipidemia, and smoking, are also prevalent in CKD. The number of people with end-stage renal disease (ESRD) is expected to rise by 50% in the next 20 years (7). In the current era, CKD is a severe health and economic burden. CKD-related mortality has increased by 82.3% in the last two decades. In addition, it has risen to third place among the world's top 25 major causes of death (8). Now, the molecular description of CKD onset and progression is lacking. Based on these findings, the researchers have described CKD as a worldwide epidemic (9). The present method for prioritizing disease-related genes is based on the "guilt-by-association" assumption, which states that physically and functionally related genes have similar phenotypic effects and are likely to be involved in the same biological pathways (10).

Network theory is a useful tool for deciphering the topological features and dynamics of complex systems and their functional modules. Many extant networks can be classified as scale-free, small world, random, or hierarchical networks. The hierarchical form of the network includes modules and sparsely dispersed hubs to manage the network which is of particular interest to biologists (11). Moreover, the identification of essential and critical protein(s) is crucial for understanding progression of the disease. Thus, the current paradigm for investigating CVD and CKD focuses on combining protein interactions, functions, and disease networks to identify important regulators of CVD and CKD among DEGs. Also, it is substantial to study network's topological characteristics, so that the essential key regulators, their function, and regulating mechanism could be forecasted

(12). The topology of a network and its many centrality measures (metrics reflecting the impact of each node within a network) can be examined and evaluated to explore fundamental biological meanings and prominent regulatory molecules (13). A network could best be studied in relation to the spreader nodes as these are projected to have the biggest impact on the process of distribution of information throughout the network because they have strong connections with other nodes. So these influential nodes can commonly be identified by calculating the characteristics like hubness and spreading potential (14). Since the fundamental characteristics of a network and its centrality metrics are universal, it can be applied to any network domain, including biological networks (15). These network centralities can be used to further narrow down and validate the extracted influential nodes. In our present study, we have used the seed genes, gene ontology, and pathways in an integrating manner to give a glimpse of molecular relation between CVD and CKD that may further facilitate the identification and validation of novel biomarkers.

METHODOLOGY

Acquisition of mRNA Expression Data

The mRNA expression profile of CVD and CKD were downloaded from the publicly available databases of gene expression microarrays, stored in the repository bank Gene Expression Omnibus (GEO) NCBI [www.ncbi.nlm.nih.gov/geo/; (16)]. These were the mRNAs expression profiles series of CVD (GSE26887, GSE42955, GSE67492, GSE71226, GSE141512, GSE48060) and CKD (GSE15072, GSE23609, GSE43484, GSE62792, GSE66494) consisting of normal and treated samples. The selection of the datasets using inclusion and exclusion criteria were made using the following keywords in the NCBI : CVD, cardiac failure, cardiac arrest, chronic heart failure (CHF), etc., whereas, CKD, AKI, chronic kidney disease, renal failure AND human [Organism] (17). The details of all GSE series are given in **Table 1**. Patient samples from various sources were not differentiated during the data integration procedure to show a common and/or overlapped gene signature. The expression microarray is a method for studying gene expression on a genome-wide scale that is widely utilized. Batch effects can be decreased through proper experimental design, but they cannot be eradicated until the entire study is conducted in one batch. Before analyzing microarray data, a few algorithms are now available to correct for batch effects. We employed the Empirical Bayes method built-in function in LIMMA, in combination with the fit2 function. Meta-analyses based on microarray data integration require effective *in silico* methods. We may now use *in silico* tools to efficiently merge numerous microarray datasets while ignoring differing demographics, experimental designs,

TABLE 1 | Samples from the GSE series and their DEGs.

SERIES	Total sample	Normal	Disease	Up regulated	Down regulated	Fold change	Illness	Country	Year	Platform	Authors	Source
GSE48060	52	21	31	15	14	0.5	CVD	USA	2014	GPL-570	Xing Li	Peripheral blood
GSE67492	6	2	4	73	16	0.5	CVD	USA	2015	GPL-6244	James West	Right ventricular wall
GSE26887	24	5	19	58	95	0.5	CVD	Italy	2012	GPL-6244	Fabio Martelli	Left ventricular wall
GSE71226	6	3	3	97	82	1.5	CVD	China	2015	GPL-570	Bofan Meng	Peripheral blood
GSE42955	29	5	24	125	236	0.5	CVD	Spain	2013	GPL-6244	M. M. Molina	Heart
GSE141512	12	6	6	69	85	0.5	CVD	Russia	2019	GPL-17586	German Osmak	Blood
GSE66494	61	8	53	102	325	0.5	CKD	Japan	2015	GPL-6480	Satohiro Masada	Kidney
GSE43484	6	3	3	134	136	0.5	CKD	Sweden	2013	GPL-571	Elham Dadfar	Uremic monocyte
GSE15072	29	8	21	51	38	2	CKD	Italy	2009	GPL-96	Palo Pontrelli	PBMC
GSE62792	18	6	12	352	262	0.5	CKD	Sri Lanka	2018	GPL-10558	D. N. Magana	Blood
GSE23609	24	7	17	219	189	0.5	CKD	USA	2010	GPL-6454	Persis P. Wadia	Serum

The entire sample available in the GSE series is shown in column 2, and the fold change values are shown in column 7. In each GSE series, the total up and down regulated genes were recorded in 5 and 6 columns, respectively. For the GSE series, the platform GPL in column 11 indicates the number of probes and the type of data (Affymetrix data and oligo data).

and specimen sources with the advancements of ever-growing theories and bioinformatics tools (18).

Identification of CVD and CKD Associated DEGs

To further analyze the obtained data samples series, the GEO2R tool (<http://www.ncbi.nlm.nih.gov/geo/geo2r/>) was used. GEO2R is a web-based analytical tool with a built-in R program and GEO query for Linear Models for Microarray Data (Limma). The default settings were utilized to prepare the datasets (19). Differentially Expressed mRNAs were extracted applying criteria $p < 0.05$ and log fold-change $|0.5-2|$ as the threshold values. Up and downregulated genes from meta-analysis were used as genes of interest in PPIN network. As a result, the Benjamini-Hochberg (BH) correction method was utilized to adjust the significant value of p obtained by the original hypothesis test during differential expression analysis. Finally, for DEGs screening, log Fold change was employed as the key index. Log fold change $|0.5-2|$ was employed as a DEG screening condition in this study. The criteria [i.e., value of $p < 0.05$ and fold change $0.5-2$] were selected in order to expand the total number of DEGs between healthy control and diseases samples. Since very few genes were differentially expressed with respect to this threshold, therefore it made the threshold more stringent and would lead to nearly no or very few DEGs. If the fold change is altered, the resulting DEGs will be changed as well, and vice versa. There is no standard value for fold change when it comes to selecting DEGs (20).

Network Construction of Protein-Protein Interactions (PPIN)

The network was built using the String online database and imported into Cytoscape v.3.8.0. It supports bipartite graph visualization of gene-gene linking/interaction/regulation (gene-disease associations) and also provides gene-centric views of the network data (21). The Probe Ids were mapped to their

corresponding gene symbols to build the native network from DEGs. The gene regulatory network of CVD and CKD was built using the simple premise of one gene and one protein. A variety of features can be used to construct and filter the network. The network combines data from curated databases with knowledge gleaned from the literature (22). Because the networks might be based on a certain gene or condition, the PPIN networks are visualized using the Cytoscape program (23). To discover the significant modules and top-ranked genes in the PPIN network, the Cytoscape plugin Molecular Complex Detection (MCODE; version 2.0.0) and the igraph with Influential packages in R (version 3.6.3) were used. The network's topological properties were estimated using Network analyzer, a Cytoscape version 3.8.0. plug-in, while the eigenvalues were generated using CytoNCA, another Cytoscape plug-in for topological properties calculation. This could also be useful for double-checking Network Analyzer data (24).

Module/Cluster/Subnetwork Finding: Molecular Complex DEtection Method

The MCODE method (A cytoscape plugin) was used to detect the modules/clusters/communities (Strongly interconnected regions) in the native network. In a PPI network, protein complexes and pathways are prevalent groupings (clusters) (25). To separate the dense regions according to provided parameters, the approach uses vertex weighting by local neighborhood density and outward traversal from a locally dense seed protein. The algorithm has the advantage of having a directed mode, which permits fine-tuning of clusters of interest without considering the remainder of the network and investigation of cluster interconnectivity, which is important in protein networks (26). The modules from the native network along with sub-modules from modules at each level of organization were identified until only motifs remained (i.e., 3 nodes with 3

edges). Vertex weighting, complex prediction, and possible post-processing to filter or add proteins in the generated complexes are the three stages of the MCODE algorithm (27). Intuitively, a network of interacting molecules can be represented as a graph with vertices representing molecules and edges representing chemical interactions. If the temporal pathway or cell signaling information is known, a directed graph with arcs reflecting chemical activity or information flow can be created. Otherwise, an undirected graph is employed. Graph theoretic methods can be used to aid in the analysis and solution of biological problems using this graph model of a biological system (28).

Gene Ontology, Pathway Analysis, and HE

Gene ontology words are a standardized set of terms separated into three categories: Molecular function, Biological Processes, and Protein Class (29). Thus, DEGs were collected and sent to ClueGO (a Cytoscape plug-in that facilitates biological interpretation and visualizes functionally grouped terms in the form of networks, tables, and charts) to enrich the given set of DEGs to possible GO terms for exploratory research. We used ClueGO to assess the function of hub genes and define the GO term. ClueGO employs kappa statistics to link the terms in the network. It creates a dynamical network structure by considering the gene lists of interest at the start. It also constructs a functionally ordered GO/pathway term network by combining GO terms and KEGG/BioCarta pathways (30). A number of adjustable limitation criteria allow for visualizations of various levels of specificity. ClueGO can also compare gene groups and highlight their functional differences. ClueGO also makes use of Cytoscape's flexible visualization framework and works in tandem with the Golorize plug-in. Gene lists can be imported directly into ClueGO or produced interactively from gene network graphs shown in Cytoscape. ClueGO comes with a few gene identities and species by default, and it is simple to add more via a plug-in. ClueGO is an open-source Java application that uses different ontologies to extract non-redundant biological information for huge clusters of genes (31).

For gene annotation and gene list enrichment analysis, Metascape leverages a variety of databases and technologies. Metascape uses lists of gene identifiers to extract rich annotations, find statistically enriched pathways, and build PPIN networks. Pathway or process enrichment analysis uses the standard accumulative hypergeometric statistical test to identify ontology words with significant input genes given a gene list (32). We give more arguably better ontology concepts, including ones from Broad's MSigDB, than other GO-based enrichment analysis tools. Modules were also subjected to MCODE to identify sub-modules and sub-sub-modules. All modules, sub-modules, and sub-sub-modules with clustering coefficients less than or equal to unity were examined. We discovered modules and sub-modules that were related to independent functions and followed the modularity laws, and the fact that their activities are non-linear (33). As a result, we needed to quantify their role as important genes at the systems biology level, which we did by utilizing HE analysis of biological networks (34).

Identification of the Most Influential Nodes Using IVI Methods

The IVI is a new method for detecting influential nodes. Hubness and spreading values combine to form the IVI algorithm. IVI captures all the network's topological dimensions. In domains ranging from transportation to biological systems, identifying critical individuals within a network is a persistent challenge. Identifying the most powerful nodes with the ability to have the most influence on the PPIN network (35), degree centrality (DC) and ClusterRank (CR), neighborhood connectivity (NC), local H index, betweenness centrality (BC), and collective influence (CI), respectively, and to synergize their effect for the unbiased identification of prominent nodes in the network (36). Influential is an R package that primarily focuses on identifying the most influential nodes in a network, as well as categorizing and rating top candidate characteristics (37).

RESULTS

Figure 1 depicts the workflow of the entire integrative network-based approach used in this study. Adobe Illustrator CS6 was used to create the flowchart.

Selection of DEGs

The GSE series of CVD denoted by X and the GSE series of CKD was denoted by Y. There are 6 GSE series of X ($X_1, X_2, X_3, X_4, X_5,$ and X_6) and 5 GSE series of Y (Y_1, \dots, Y_5).

$$Xu = (X_1u_1, X_2u_2, \dots, X_6u_6) \quad (1)$$

where u stands for upregulation.

$$Xd = (X_1d_1, X_2d_2, \dots, X_6d_6) \quad (2)$$

d stands for downregulation.

$$Yu = (Y_1u_1, \dots, Y_5u_5) \quad (3)$$

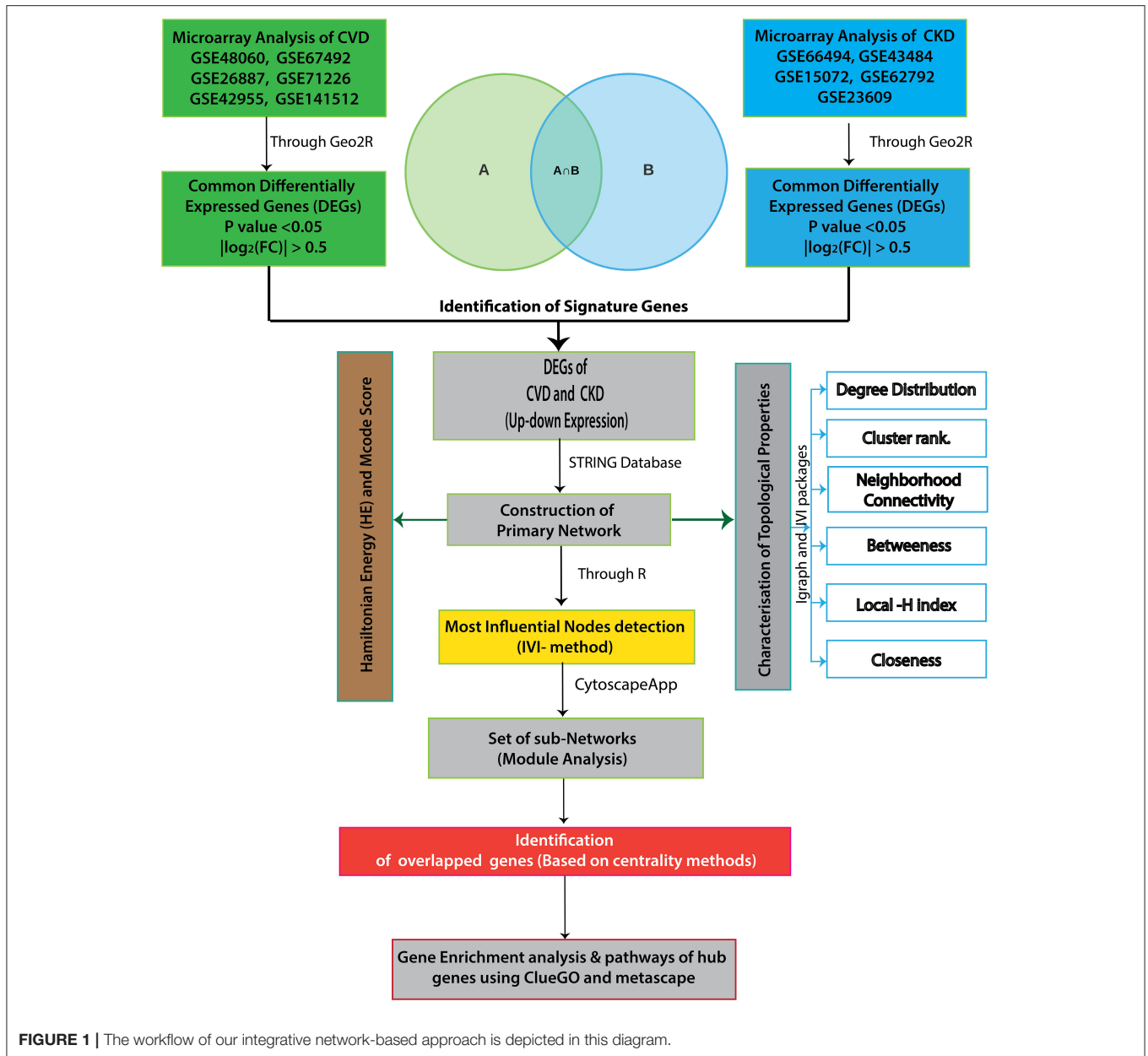
$$Yd = (Y_1d_1, \dots, Y_5d_5) \quad (4)$$

To find DEGs, we combine equations, i.e., (1) with (3) and (2) with (4), as follows:

$$Xu \cap Yu = \{Xu\} \cap \{Yu\} \quad (5)$$

$$Xd \cap Yd = \{Xd\} \cap \{Yd\} \quad (6)$$

The intersection of (5) and (6) gives the Overlapped genes. Genes showing a value of $p \leq 0.05$ and $\log \text{fold change } |0.5-2.0|$ were considered statistically significant and differentially expressed. The total upregulated genes in all 11 GSE series of CVD and CKD was $Xu \cap Yu = \{1295\}$, whereas total downregulated genes are $Xd \cap Yd = \{1478\}$. Total up and downregulated genes in CKD and CVD, separately, are 437 and 528, and 858 and 950 while the total upregulated genes in all 11 GSE series of CVD and CKD are 1,295, and downregulated genes are 1478 (**Table 2**). After comparison of CVD vs. CKD, we finally got 43 overlapped genes, including 24 upregulated genes in CVD and CKD, and 19 genes downregulated in both diseases (**Figure 2**).



Gene Network Construction

Based on mRNA profiling and protein networks, to generate subnetwork biomarkers (interconnected genes whose aggregate expression levels are predictive of disease state), networks provide a rich source of biomarkers for illness classification. To construct a CVD and CKD interaction network and infer gene-disease correlations using network features (38), we started with a list of seed/key genes (43 DEGs) that are known to be associated to the disease, and each gene is represented by a single node in the interaction network. Next, we built a disease-specific gene-interaction network where the nodes are the genes and the edges are their connections (39) using selection of top ranked genes

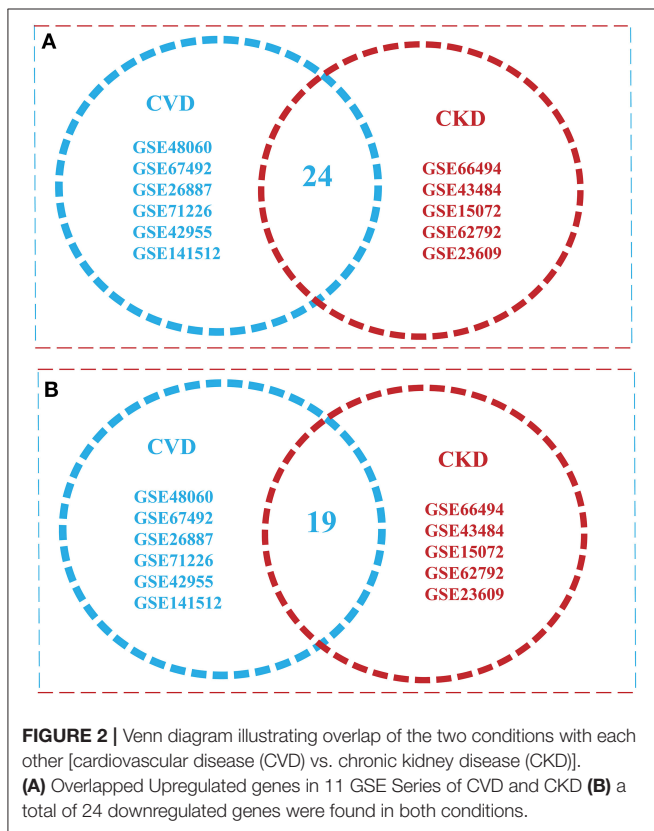
in the network via IVI -Value, Spreading score, Hubness score, ClusterRank, Collective influence, h-index, Local h-index degree centrality (D_C), betweenness centrality (B_C), and Neighborhood Connectivity (N_K) centrality metrics.

A network representation and analysis is a powerful tool for studying the complicated behavior of biological systems' physiology and pathology (40). Through cluster/module analysis, it was studied that the CVD and CKD network shows hierarchical scale free nature. The 19 key genes and their presence in various modules are traced following MCODE community finding algorithm. There are 15 modules (highly connected nodes) extracted from the native network. Ten out of 15 modules were

TABLE 2 | The up and downregulated genes are listed in a table with a count number column.

Sr. No.	Common genes in CVD and CKD	# Count	Gene symbol
1	UP regulation	19	NPR3, NFE2L1, TNFSF10, HMGB2, GABPB2, KDM5D, RSRP1, GPCPD1, ZNF83, THY1, COX7B, NPPB, PDZK1IP1, BCL6, IRAK3, GRN, SOCS3, CASP5, RPS24
2	Down regulation	24	BCL3, ZRANB2, NR1D2, C7, LYN, ANXA3, PER3, PTP4A3, RPLP0, HSPB1, ACTG1, RPL13, HCAR3, FCGR3A, MAP2K3, MYC, CIRBP, AHS2, ATP1A1, NPIP3, PNISR, RPS2, ENO1, CNN1

Up-regulated genes have red lettering, whereas downregulated genes have green text.



found to be having our seed genes (Figure 3). These genes will be utilized to build a gene network and to investigate their biological importance.

Gene Enrichment Analysis and Pathways

The key genes are submitted to ClueGO a cytoscape plugin to find the Gene Ontology term. The default setting of ClueGO are network specificity (medium), organism (human), visuals styles (group), evidence of experiments, all experimental (EXP, IDA, IPI, IMP, IGI, and IEP), and value of $p < 0.05$ (41). ClueGO

constructs a functionally ordered GO/pathway term network by combining Gene Ontology (GO) terms and KEGG/BioCarta pathways. It can evaluate and compare numerous lists of genes and visualize functionally grouped terms in a comprehensive way. ClueGO can be used in conjunction with the Golorize plug-in to offer an intuitive depiction of the analysis results. ClueGO is enhanced with CluePedia, which allows for a thorough examination of pathways (42). WikiPathways is a collaborative, open-source tool for curating biological pathways. Metascape selects the most informative phrases from the GO clusters obtained using a heuristic method. It takes a sample of the 20 highest-scoring clusters, picks up to 10 best-scoring words (lowest p -values) inside each cluster, and then connects all term pairs with Kappa similarity >0.3 (Figure 4). Cytoscape is used to show the resulting network, with each node representing one enriched phrase. The cluster IDs or the p -values can be used to color the nodes. Edges connect phrases that are similar—the thicker the edge, the greater the resemblance (43). To maintain readability, only one label (corresponding to one term) is displayed per cluster (Figure 4).

Hamiltonian Energy

$$HE = E_c - \gamma N_c,$$

where E_c represents number of edges in a cluster, N_c for number of nodes, and the gamma constant $\gamma = 0.8$. The HE calculation for a network within the modules considers contributions from the organization of nodes and edges in a competitive manner, and this energy is used in organizing or re-organizing the network at various levels. This approach can also magnify the significant changes in the network organization when it goes down to various levels of organization, which capture the importance of hubs in the network and at the modular level. Therefore, HE formalism proves to be a useful technique for considering variations in the network organization (44). For hubs at each level of all potential modules in the network, the HE was determined (Figure 2). When the network's HE is plotted as a function of network modules, we discover that the energy distribution is highest in the native network and gradually decreases as the amount of organization grows. Because HE is based on node and edge competition for a set resolution parameter value (gamma symbol), a drop in HE reflects the dominance of interacting edges over the network size, implying rapid information processing (45).

Most Influential, Potential, and Sovereignty of the Nodes in a Network

Integrated Value of Influence (IVI) is a method for identifying the most influential nodes in a network that considers all topological aspects. The IVI formula combines the most important local (degree centrality and Cluster Rank), semi-local (neighborhood connectivity and local H-index), and global (betweenness centrality and collective influence) centrality measures in such a way that their effects are synergized and their biases are eliminated (46). The degree function from the igraph package can be used to calculate degree centrality, which is the most used local

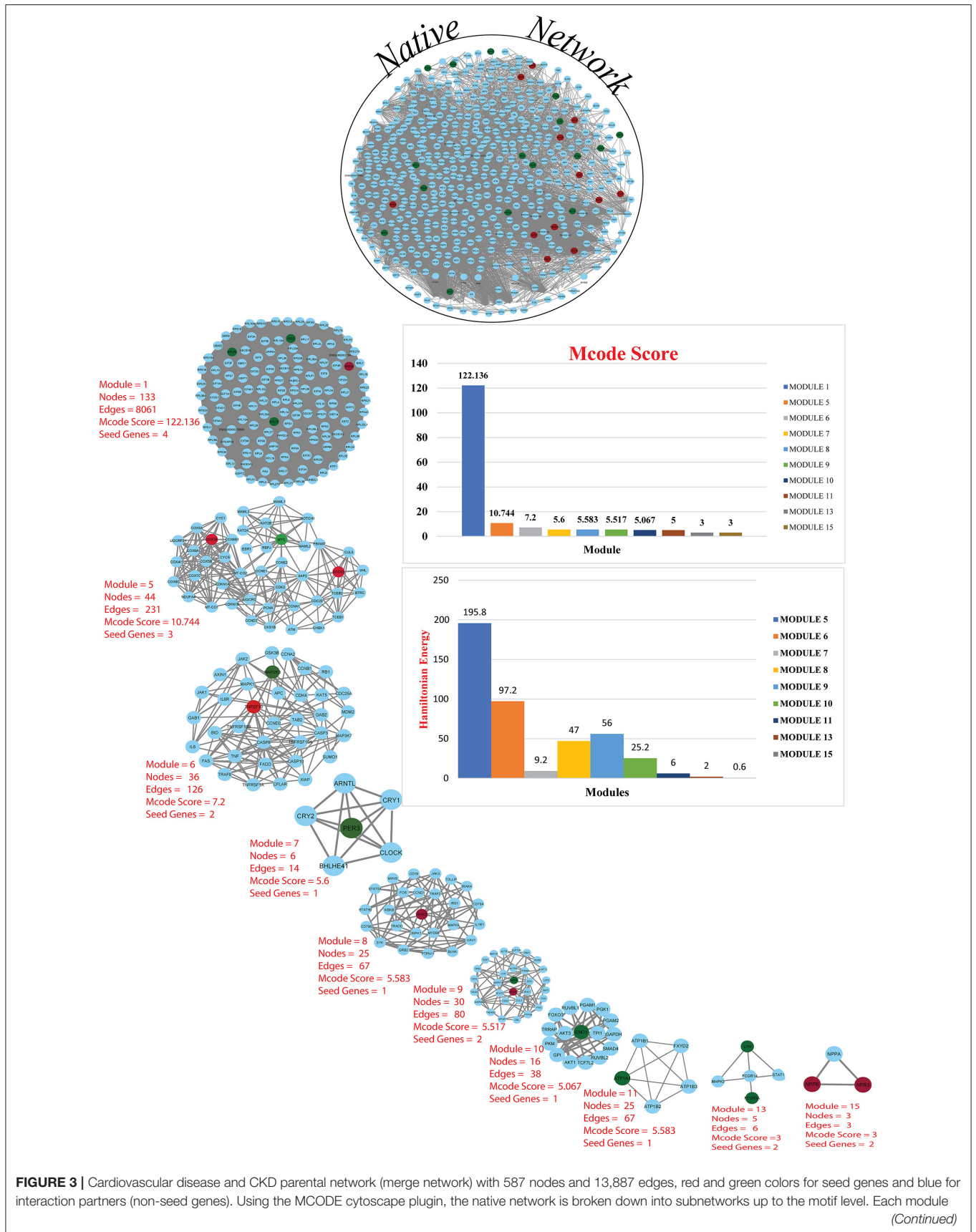
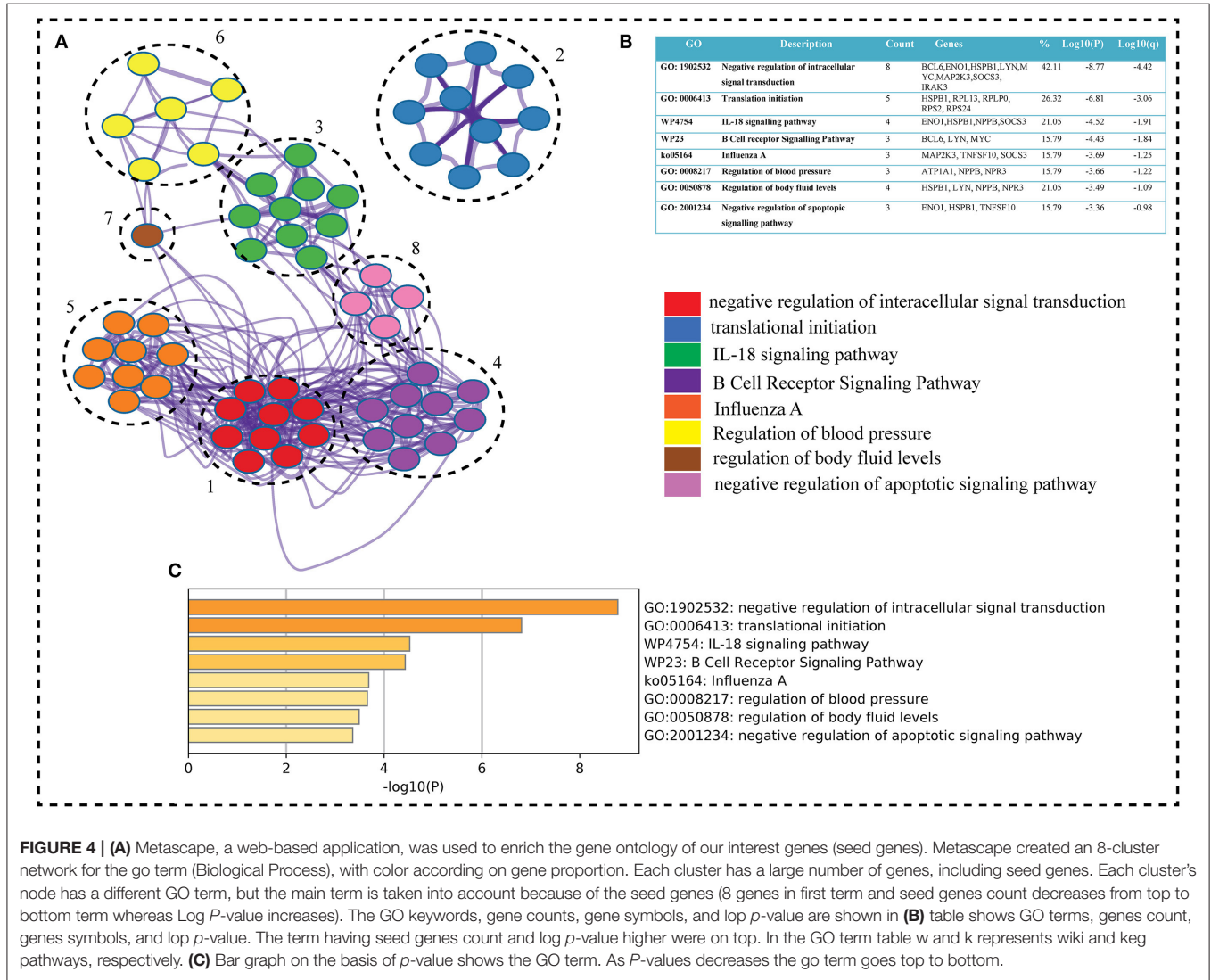


FIGURE 3 | Cardiovascular disease and CKD parental network (merge network) with 587 nodes and 13,887 edges, red and green colors for seed genes and blue for interaction partners (non-seed genes). Using the MCODE cytoscape plugin, the native network is broken down into subnetworks up to the motif level. Each module (Continued)

FIGURE 3 | subnetwork from native network represents with MCODE score and seed genes (up-regulated red and downregulated green). The hierarchy of energy is depicted on the right side of the illustration by a Hamiltonian energy (HE) bar graph. As the number of nodes in the modules decreases, so does the amount of energy used. The HE was calculated for nodes at each level of all conceivable modules in the network. The HE of the CVD and CKD networks is given as a function of network levels. We determined that energy distribution is greatest in the core network and diminishes as the level of (modules) organization increases. Because HE is dependent on nodes and edges for a fixed resolution parameter value ($\gamma = 0.8$), the drop in HE shows the dominance of interacting edges over the network size, indicating rapid information processing. The HE of a complex network is a measure of overall energy in the system, and its value fluctuates as the network structure changes.



centrality measure. The degree centrality (DC) $DC_i = \sum_{i \neq j} A_{ij}$ is the simplest local centrality metric for a graph, where A represents the adjacency matrix of the associated network and $A_{ij} = 1$ if nodes i and j are connected and $A_{ij} = 0$, otherwise (47). Betweenness centrality, like degree centrality, is a widely used centrality metric. However, it only represents a node's global centrality. Another important centrality metric that reflects a node's semi-local centrality is neighborhood connectedness. For the first time, this centrality measure can be calculated in the R environment using the influential package. ClusterRank is

another local centrality metric that removes the negative impacts of local clustering by intermediating between local and semi-local properties of a node. The H-index is a measure of how well a piece of the H-index is a semi-local centrality metric that was inspired by its use in analyzing the influence of researchers and is now available in the R environment for the first time via the influential package (48). Local H-index (LH-index) is a semi-local centrality measure and an upgraded variant of H-index centrality that applies the H-index to a node's second order neighbors and is now calculable in R using the influential package. The product of

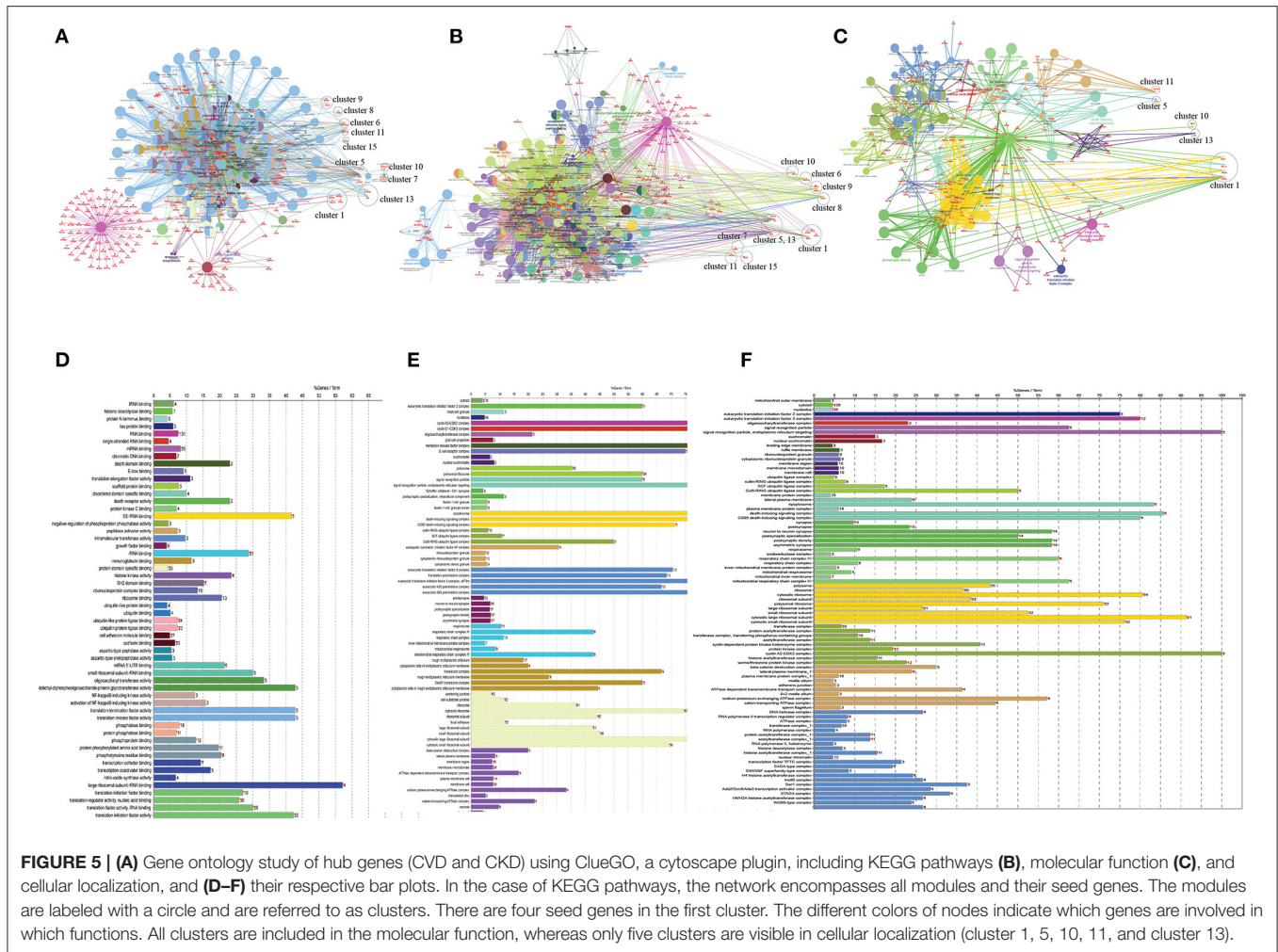


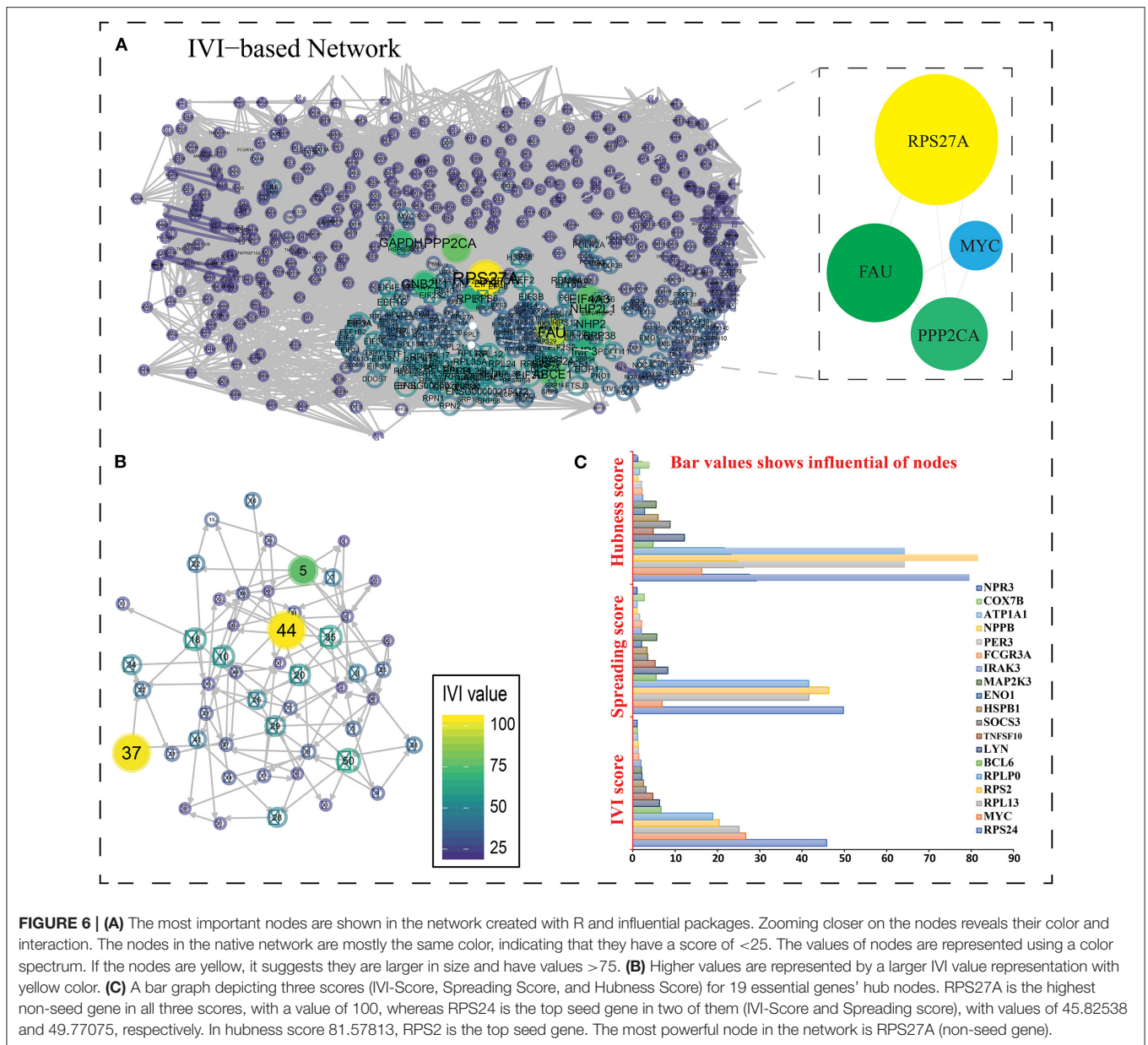
FIGURE 5 | (A) Gene ontology study of hub genes (CVD and CKD) using ClueGO, a cytoscape plugin, including KEGG pathways (B), molecular function (C), and cellular localization, and (D–F) their respective bar plots. In the case of KEGG pathways, the network encompasses all modules and their seed genes. The modules are labeled with a circle and are referred to as clusters. There are four seed genes in the first cluster. The different colors of nodes indicate which genes are involved in which functions. All clusters are included in the molecular function, whereas only five clusters are visible in cellular localization (cluster 1, 5, 10, 11, and cluster 13).

TABLE 3 | The gene tracing in a network where the primary network is broken down into subnetworks/clusters/modules is shown in this table.

Sr. No.	Module	Nodes	Edges	#Count	Gene of interest
1	Module 1	133	8061	4	RPL13, RPLP0, RPS2, RPS24
2	Module 5	44	231	3	MYC, COX7B, SOCS3
3	Module 6	36	126	2	MAP2K3, TNFSF10
4	Module 7	6	14	1	PER3
5	Module 8	25	67	1	IRAK3
6	Module 9	30	80	2	BCL6, HSPB1
7	Module 10	16	38	1	ENO1
8	Module 11	5	10	1	ATP1A1
9	Module 13	5	6	2	LYN, FCGR3A
10	Module 15	3	3	2	NPR3, NPPB

Ten modules out of fifteen have our gene of interest (seed genes). The table displays the number of nodes, edges, and genes in the specific module. Upregulation genes are shown in red, whereas downregulation genes are highlighted in green. There are a total of 19 genes that have been traced (11 downregulation and 8 up-regulation).

the reduced degree (degree – 1) of a node and the total reduced degree of all nodes at a distance d from the node is calculated as Collective Influence (CI). For the first time, this centrality metric is included in a R package. Two global centrality measures, betweenness centrality and collective influence, are among the most extensively used for identifying network influencers. Betweenness is the likelihood of a node in a network to be on the shortest path between nodes. Influencers of information flow inside a network are nodes with a high betweenness. Sometimes, we want to find the nodes that have the most potential for propagating information throughout the network, rather than the most influential nodes. ClusterRank, neighborhood connectedness, betweenness centrality, and collective impact all contribute to the spreading score, which is an integrative score made up of four separate centrality measurements. Also, one of the primary components of the IMI is the spreading score, which measures the spreading potential of each node within a network. In some circumstances, we wish to find out which nodes have the most sovereignty in their immediate surroundings. Hubness score is an integrative score comprised of two different centrality



measures: degree centrality and local H-index (49). In addition, the Hubness score, which is one of the key components of the IVI, shows the power of each node in its surrounding environment (Figure 5).

DISCUSSION

The risk of CVD is increased with stages of CKD by promoting myocardial hypertrophy, coronary (CAD), atherosclerosis, and fluid overload. As the two most important organs of the body, the heart and kidneys work in close relation to each other. So, to unroll this methodical relationship at the molecular level, the present study was intervened. In this study, we have used integrated network-based approach and IVI methods to extracts

the information (influential of nodes), hub genes, functions, and pathways. One of the limitations of this kind of study is that we have different cell and tissue types. Using p-adjustment is not the right choice under such circumstances as we did get no significant genes at 0.5 adjusted *P*-value for the GSE43484 and GSE67492. The current study is more like the meta-analysis of gene expression datasets using common microarray platforms which is quite widespread in many species. Apart from all the technicalities, the sharing of similar functions associated with transcripts of similar expression has persistently been used to annotate functions for humans in bioinformatics. Thus, using multiple datasets within functional premises governed by genes expressing in cell/tissue for a phenotype can be considered to involve similar pathways. This study retrieved 2,773 DEGs from

TABLE 4 | The top 20 nodes in the network were extract on the basis of IMI-score, spreading score, hubness score, CI score, and local HI score.

Sr. No.	Gene	IMI-value	Gene	Spreading score	Gene	Hubness score	CI	Gene	Local HI	Gene
1	RPS27A	100	RPS27A	100	RPS27A	100	1453138	EIF4G1	19288	RPS27A
2	FAU	86.54204	UBA52	66.35965	UBA52	83.6756	919132	FAU	17854	UBA52
3	PPP2CA	69.49985	EIF2S2	53.61083	RPS6	82.12102	910888	RPL10	17813	RPS6
4	EIF4A3	66.75017	EIF3M	53.49261	RPS2	81.57813	897390	RPL10A	17813	RPS2
5	ABCE1	65.97182	EIF3C	53.38627	RPS7	81.44018	866059	RPL10L	17792	RPS14
6	NHP2L1	64.97156	EIF3J	53.20541	RPS9	81.44018	862729	RPL11	17761	RPS7
7	GAPDH	61.76868	EIF2S1	53.19844	RPS14	81.30669	816804	RPL12	17692	RPS9
8	GNB2L1	60.52372	EIF3D	52.99297	RPS3	80.93769	806190	RPL13	17649	RPS3
9	IMP3	56.46971	EIF3K	52.99297	RPS18	80.63545	774473	RPL13A	17606	RPS11
10	NHP2	56.35967	EIF3B	52.53035	RPS11	80.50452	769952	RPL14	17606	RPS18
11	RPL11	55.67579	EIF5	52.38929	RPS27	80.35306	761514	RPL15	17606	RPS27
12	RPP38	51.82545	EIF3F	52.28384	RPS13	80.3332	751443	RPL17	17606	RPS13
13	EIF3D	46.9192	EIF3H	52.28384	RPS16	80.3332	681471	RPL18	17606	RPS15
14	RPS24	45.82538	EIF1AX	52.28095	RPS17	80.3332	674001	RPL18A	17606	RPS16
15	EEF1G	45.05756	PPP2CA	51.95736	RPS23	80.3332	646646	RPL19	17606	RPS17
16	BOP1	44.26816	RPS14	51.83609	RPS3A	80.3332	634176	RPL21	17606	RPS23
17	EIF3L	43.55821	RPS7	51.10068	RPS4X	80.3332	630175	RPL22	17598	RPS3A
18	RPL24	42.99506	RPS9	51.10068	RPS5	80.3332	624200	RPL22L1	17584	RPS4X
19	RPL14	42.20691	GNB2L1	50.96442	RPS8	80.3332	622336	RPL23	17548	RPS5
20	RPS28	41.40638	SEC61B	50.94699	RPS15	80.27672	621550	RPL23A	17548	RPS8

These 20 nodes/genes are the most important nodes in the network retrieved from IMI methods. Using versatile methods (IMI-methods), most influential network nodes can be detected.

11 GSE Series (6 CVD and 5 CKD) series with thousands of genes. The 2,873 genes were overlapped in both cases during the process of distinguishing between the significant genes. Finally, based on our filtering criterion, we got to 43 key (or seed) genes in both conditions (24 down and 19 up-regulated genes) represented by Venn diagram in **Figure 2**.

Our retrieved key genes might be of significance in understanding the pathological degree of CRS in a better way. The network was constructed from 43 seed genes (487 nodes and 12,027 edges) using String (a web tools) with an interaction score of 0.9, the network was then imported to Cytoscape (3.8.1) for further downstream analysis. Out of 43, only 19 seed genes (8 up and 11 downregulated genes) were retained by the native network.

To find the involvement of the DEG(s) at different levels in the constructed network, the native or primary network was further broken down to 15 subnetworks or modules using MCODE (MCODE parameters were used for network scoring and cluster finding, i.e., “Degree cutoff = 2,” “node score cutoff = 0.2,” “k-score = 2,” and “max. depth = 100.” Out of these 15 modules, 10 modules were found to have seed genes. Interestingly, Module 1 contains 4 downregulated (RPL13, RPLP0, RPS2) and one upregulated (RPS24) gene, module 5 contains one downregulated gene (MYC) and two (SOCS3, COX7B) upregulated genes, module 6 contains two genes, one (MAP2K3) downregulated and one (TNFSF10) up-regulated gene. Modules 7 and 8 consist of one downregulated (PER3) and one (IRAK3) up-regulated gene. Module 9 contains two genes, one BCL6 (upregulated) and one HSPB1 (downregulated). Module 10 contains one downregulated gene (ENO1). Module 11 contains the gene

ATP1A1 (downregulated), and module 13 and 15 contain two genes each, namely, LYN, FCGR3A (downregulated) and NPR3, NPPB (up-regulated) as shown in **Table 3**. As the number of nodes and edges decreases, the MCODE score decreases as shown in **Figure 3**. A high MCODE score indicates that the nodes are well-connected (dense network). To further establish the stability and integrity of these modules, Hamiltonian energy was calculated using the formalism in the method section where low HE suggests less likely to remain stable under stress (say when seed genes are removed). Module 7 shows very low value of HE, while modules 8 and 9 bar indicate higher values than module 5 (see **Figure 3**). The decline of top to bottom indicates the hierarchy of nodes. Seed genes (19) were further studied for their functions (GO TERM) and pathways. These 19 genes were submitted to Metascape, an online database, to get an understanding of the biological processes, molecular functions, and pathways they represent. Gene ontology terms are a comprehensible input of terms organized into three categories: Molecular function, Biological Processes, and Protein Class. Thus, these extracted DEGs were submitted to ClueGO, a Cytoscape plug-in that facilitates the biological interpretation, functional differences, and visualizes functionally grouped terms in the form of networks, tables, and charts (**Figure 4**). It illustrates the clusters of 8 networks based on the color of the gene connections and the percentage of genes in each cluster. The seed gene count, *p*-value, and gene symbol, along with their GO-TERM are represented in the table.

Based on GO term enrichment, the highest represented a group of 8 genes (BCL6, ENO1, HSPB1, LYN, MYC, MAP2K3, SOCS3, and IRAK3) perform negative regulation of intracellular

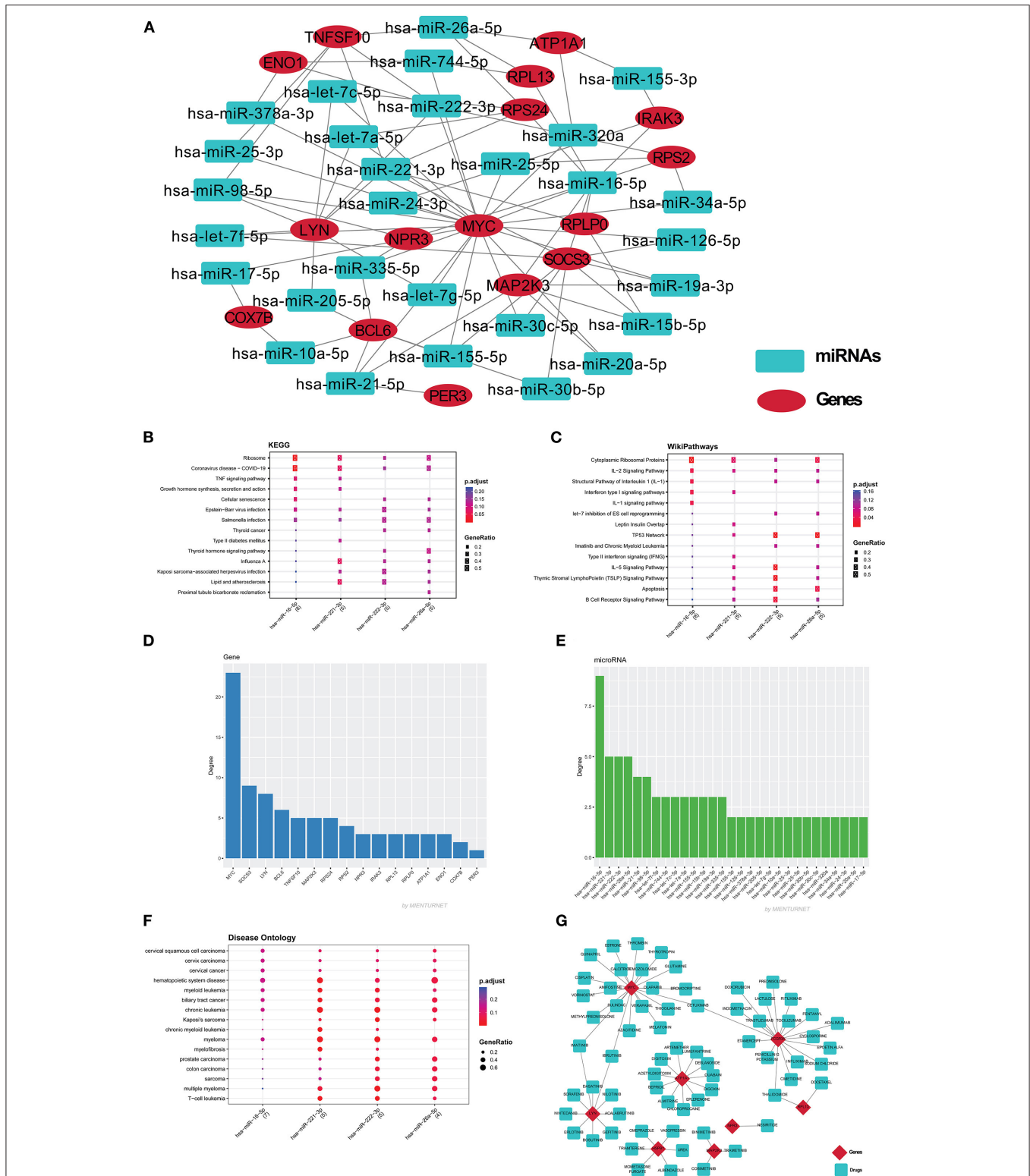


FIGURE 7 | (A) The miRNAs-mRNA network contains 47 nodes and 85 edges. Red color eclipse indicates genes, whereas, cyan color rectangle indicates their associated miRNAs. The mienturnet database also analyzes the major miRNAs pathways of key miRNAs. The degree of these four miRNAs was plotted against the KEGG pathways **(B)**, WikiPathways **(C)**, and disease ontology **(F)**. The bar plot shows the genes **(D)** and miRNA **(E)** based on degree centrality. **(G)** The gene-drug network was build using drug gene interaction database, which build the network of 78 nodes and 72 edges. Red color diamond for genes and cyan color for their drugs.

TABLE 5 | The scores of the 19 seed genes in the native network were determined.

Sr. No.	Gene	IVI score	Gene	SPD score	Gene	Hubness score
1	RPS24	45.82538	RPS24	49.77075	RPS2	81.57813
2	MYC	26.69248	RPS2	46.32048	RPS24	79.5567
3	RPL13	25.10682	RPL13	41.60822	RPL13	64.30335
4	RPS2	20.43554	RPLP0	41.56268	RPLP0	64.30078
5	RPLP0	18.87599	LYN	8.263571	MYC	16.28468
6	BCL6	6.661571	MYC	6.925186	LYN	12.20791
7	LYN	6.297702	MAP2K3	5.662946	SOCS3	8.827513
8	TNFSF10	4.720607	BCL6	5.502842	HSPB1	5.966899
9	SOCS3	3.093086	TNFSF10	5.278298	MAP2K3	5.497646
10	HSPB1	2.515714	SOCS3	3.546049	TNFSF10	4.816811
11	ENO1	2.15667	HSPB1	3.370381	BCL6	4.770602
12	MAP2K3	2.067014	COX7B	2.702907	COX7B	3.981947
13	IRAK3	1.913351	FCGR3A	2.099974	ENO1	2.789033
14	FCGR3A	1.432519	ENO1	2.067738	IRAK3	2.3437
15	PER3	1.328185	IRAK3	2.014448	FCGR3A	2.182645
16	NPPB	1.24651	PER3	1.614294	PER3	2.082526
17	ATP1A1	1.15923	ATP1A1	1.031002	ATP1A1	1.611522
18	COX7B	1.088852	NPPB	1	NPPB	1.19186
19	NPR3	1.030828	NPR3	1	NPR3	1.19186

RPS24 has the greatest score in the table, while NPR3 has the lowest.

signal transduction (GO:1902532) while the least suggested function is negative regulation of apoptotic signaling pathway (GO:2001234) (see **Figure 5A** for seed gene pathways), with circles indicating modules. The different pathways are indicated by the color of interaction between nodes. If a gene has multiple colors, it suggests that it plays multiple roles in different pathways. Genes that play a key role in the pathophysiology of various diseases could be useful biomarkers in future research. In cluster 5, the gene MYC has many colors and various connections via edges. Thus, it may be a more important gene as compared to others. While some seed genes, like RPS24 and RPS2, show only one type of color that suggests a unique function that also plays a key role (see **Figures 5B,C** for molecular functions and cellular location of seed genes). Following the PPIN and Gene enrichment analyses, we tried to find the most influential nodes, also known as hub nodes, using the IVI-value and other associated scores. The IVI values, hubness score, spreading score, and local HI index of the 19 seed nodes are displayed in the network. The non-seed genes, such as RPS27A and FAU, have the greatest values. In **Figure 6**, the size of the nodes and colors indicates higher to lower IVI value. If the nodes have a higher value than 100, the color will be yellow and circle size enlarge. The exact IVI-value of nodes is mentioned in **Table 4**. The spreader nodes are projected to have the largest impact on the flow of information throughout the network because they have high connections with other nodes inside the network. We took these influential nodes to add one more intermediate layer of information in the networks that reveal the interaction of genes and proteins through the intermediate miRNA that regulate the genes (**Figure 7**). Thus, giving us a glimpse of the underlying

physiology of these two conditions that were cumulatively called CRS.

Furthermore, we used various other available tools for identifying the most influential nodes with IVI like based on its centrality measurements (9, 10). The DC is the simplest local centrality measure for a graph (degree centrality). Two global centrality measures, betweenness centrality, and collective influence, are among the most extensively used for identifying network influencers. Betweenness is the tendency of a node in a graph to be on the shortest path between nodes (1). Influencers of information flow inside a network are nodes with a high betweenness (11). The collective number of nodes that may be reached from a given node is measured by collective impact, a new global centrality metric. Neighborhood connectedness is a network's semi-local centrality measure that considers node connectivity (number of neighbors). It's called a semi-local measure because it's not limited to a node's immediate neighbors and considers the entire environment. The average connectivity of all neighbors of a vertex I is defined as its neighborhood connectivity. It is also said that a node's prominence in the network is determined by not only the number of first connections (degree centrality), but also the amount to which the nodes near neighbors are connected to each other and other nodes (neighborhood connectivity). The greatest value h such that there are at least h neighbors of a degree greater than or equal to h is defined as the H index of node i . The local H index is a semi-local centrality metric, despite its name, because it applies the H index centrality to a node's second order neighbors. All these centrality metrics (Hubness Score, Spreading Score, Degree Centrality, ClusterRank, local H index, neighborhood connectivity, betweenness centrality, and collective influence)

are critical for identifying a network's most significant nodes (Table 5). Based on five centrality top 20 genes network extract from native network (Figure 8).

These results offer DEGs that may act as therapeutic targets for CVD and CKD in the future. This study reveals many aspects of CVD and CKD, such as gene-gene interaction, gene enrichment analysis, and pathways of hub genes. The hub genes may be the biomarker of the two conditions (CVD and CKD) need to be validated further but there are limitations such as few genes may be up-regulated and downregulated in the separate entity (means either in CVD or CKD). Maybe those genes are the key genes in CVD or CKD further research will reveal this gap. The study mainly focuses only on overlapped genes, despite all up and down genes. The non-seed genes are the most influential nodes in the network, not related to CVD and CKD. Because of the PPIN networks from the String database construct, the gene-gene interaction network using the source selected (human) and not disease specific genes interact with the seed genes. So, the study focuses only on the seed genes or related genes with the disease, but the results show the IVI -score, hubness score, and Spreading score, etc., of the non-seed genes (Table 4).

Our computational approach offers a comprehensive study, revealing the biomarkers of CVD and CKD using network approach and IVI methods (centrality measures), signifying the importance of nodes in the network, which help in Discover and understanding the various aspects of this disease. CKD Patients exhibit a pronounced risk for CVD events, utmost 50% of patients with CKD (stage 4 to 5) have CVD.

CONCLUSION

Evidence-based approach has always been the center of clinical studies, while *in-silico* approaches focus to produce that potential evidence based on past knowledge, thus making this integrated process fast and efficient. On the other hand, there is great efforts are ongoing with the aim of reducing CVD residual risk by developing reliable prognostic and predictive biomarkers. Apart from many challenges, finding seed genes is one of the first challenges and we have proposed a very simple and efficient way to do that using set theory. The resulting 43 seed genes (that defines the molecular relationship between CVD and CKD) can then be used to construct the GGiN (gene-gene interaction network) to uncover the possible biological and functional meaning. On the other hand, we have used IVI method

to calculate the influence of the nodes in the network, which further minimizes the gene list to a more realistic one (that can be tested *in-vivo* or *vitro*). Our study finds 19 genes out of many for being more prominent in the CRS (published data), whereas many other genes show a good expressions level. Although, RPS27A, a non-seed gene, was found to be the most influential node in the network followed by RPS2 and MYC. Based on these findings, new validation experiments can be constructed to further prove these as markers or good drug targets. Thus, giving us an opportunity to reduce the risks of CKD and CVD.

DATA AVAILABILITY STATEMENT

The datasets presented in this study can be found in online repositories. The names of the repository/repositories and accession number(s) can be found in the article/Supplementary Material.

AUTHOR CONTRIBUTIONS

MA and RI conceptualized the work. MA and AA did data curation. MA, RA, SH, and AS prepared the figures. MA, RA, ST, AA, SA, and RI wrote the manuscript. HB, SA, MA, RI, and RB revised the manuscript. All authors contributed to the article and approved the submitted version.

FUNDING

MA, ST, and RA were financially supported by the Indian Council of Medical Research, Government of India under Senior Research Fellow. FTS No. ISRM 11/(04)/2019. AA financially was supported by the Department of Health and Research, (DHR) Ministry of Health and Family Welfare, Government of India under young scientist F.No. 12014/06/2019-HR.

SUPPLEMENTARY MATERIAL

The Supplementary Material for this article can be found online at: <https://www.frontiersin.org/articles/10.3389/fcvm.2021.755321/full#supplementary-material>

Supplementary Table 1 | In cardiovascular disease (CVD) and chronic kidney disease (CKD), total DEGs were gathered from 11 GSE series, as well as up and down common genes.

Supplementary Table 2 | All genes rank order via Integrated Value of Influence (IVI) values.

REFERENCES

- Jankowski J, Floege J, Fliser D, Böhm M, Marx N. Cardiovascular disease in chronic kidney disease: pathophysiological insights and therapeutic options. *Circulation*. (2021) 143:1157–72. doi: 10.1161/CIRCULATIONAHA.120.050686
- Webster AC, Nagler EV, Morton RL, Masson P. Chronic kidney disease. *Lancet*. (2017) 389:1238–52. doi: 10.1016/S0140-6736(16)32064-5
- Rysz J, Gluba-Brzózka A, Rysz-Górzynska M, Franczyk B. The role and function of HDL in patients with chronic kidney disease and the risk of cardiovascular disease. *Int J Mol Sci*. (2020) 21:601. doi: 10.3390/ijms21020601
- Carracedo J, Alique M, Vida C, Bodega G, Ceprián N, Morales E, et al. Mechanisms of cardiovascular disorders in patients with chronic kidney disease: a process related to accelerated senescence. *Front Cell Dev Biol*. (2020) 8:185. doi: 10.3389/fcell.2020.00185
- Saritas T, Floege J. Cardiovascular disease in patients with chronic kidney disease. *Herz*. (2020) 45:122–8. doi: 10.1007/s00059-019-04884-0

6. Kelly DM, Rothwell PM. Does chronic kidney disease predict stroke risk independent of blood pressure? A systematic review and meta-regression. *Stroke*. (2019) 50:3085–92. doi: 10.1161/STROKEAHA.119.025442
7. Pálsson R, Patel UD. Cardiovascular complications of diabetic kidney disease. *Adv Chronic Kidney Dis*. (2014) 21:273–80. doi: 10.1053/j.ackd.2014.03.003
8. Murray CJL. The state of US health, 1990–2010: burden of diseases, injuries, and risk factors. *JAMA*. (2013) 310:591–606. doi: 10.1001/jama.2013.13805
9. Romagnani P, Remuzzi G, Glasscock R, Levin A, Jager KJ, Tonelli M, et al. Chronic kidney disease. *Nat Rev Dis Primer*. (2017) 3:17088. doi: 10.1038/nrdp.2017.88
10. Wang X, Gulbahce N, Yu H. Network-based methods for human disease gene prediction. *Brief Funct Genomics*. (2011) 10:280–93. doi: 10.1093/bfgp/eln024
11. Simpson SL, Bowman FD, Laurienti PJ. Analyzing complex functional brain networks: fusing statistics and network science to understand the brain. *Stat Surv*. (2013) 7:1–366. doi: 10.1214/13-SS103
12. Joshi A, Rienks M, Theofilatos K, Mayr M. Systems biology in cardiovascular disease: a multiomics approach. *Nat Rev Cardiol*. (2021) 18:313–30. doi: 10.1038/s41569-020-00477-1
13. Salavaty A, Ramialison M, Currie PD. Integrated value of influence: an integrative method for the identification of the most influential nodes within networks. *Patterns*. (2020) 1:100052. doi: 10.1016/j.patter.2020.100052
14. Meghanathan N. Neighborhood-based bridge node centrality tuple for complex network analysis. *Appl Netw Sci*. (2021) 6:47. doi: 10.1007/s41109-021-00388-1
15. Ashtiani M, Salehzadeh-Yazdi A, Razaghi-Moghadam Z, Hennig H, Wolkenhauer O, Mirzaie M, et al. A systematic survey of centrality measures for protein-protein interaction networks. *BMC Syst Biol*. (2018) 12:80. doi: 10.1186/s12918-018-0598-2
16. Devarbhavi P, Telang L, Vastrad B, Tengli A, Vastrad C, Kotturshetti I. Identification of key pathways and genes in polycystic ovary syndrome via integrated bioinformatics analysis and prediction of small therapeutic molecules. *Reprod Biol Endocrinol*. (2021) 19:31. doi: 10.1186/s12958-021-00706-3
17. Prashanth G, Vastrad B, Tengli A, Vastrad C, Kotturshetti I. Investigation of candidate genes and mechanisms underlying obesity associated type 2 diabetes mellitus using bioinformatics analysis and screening of small drug molecules. *BMC Endocr Disord*. (2021) 21:80. doi: 10.1186/s12902-021-00718-5
18. Fajarda O, Duarte-Pereira S, Silva RM, Oliveira JL. Merging microarray studies to identify a common gene expression signature to several structural heart diseases. *BioData Min*. (2020) 13:8. doi: 10.1186/s13040-020-00217-8
19. Mou T, Zhu D, Wei X, Li T, Zheng D, Pu J, et al. Identification and interaction analysis of key genes and microRNAs in hepatocellular carcinoma by bioinformatics analysis. *World J Surg Oncol*. (2017) 15:63. doi: 10.1186/s12957-017-1127-2
20. Afroz S, Giddaluru J, Vishwakarma S, Naz S, Khan AA, Khan N. A comprehensive gene expression meta-analysis identifies novel immune signatures in rheumatoid arthritis patients. *Front Immunol*. (2017) 8:74. doi: 10.3389/fimmu.2017.00074
21. Pavlopoulos GA, Kontou PI, Pavlopoulou A, Bouyioukos C, Markou E, Bagos PG. Bipartite graphs in systems biology and medicine: a survey of methods and applications. *GigaScience*. (2018) 7:giy014. doi: 10.1093/gigascience/giy014
22. Szklarczyk D, Morris JH, Cook H, Kuhn M, Wyder S, Simonovic M, et al. The STRING database in 2017: quality-controlled protein-protein association networks, made broadly accessible. *Nucleic Acids Res*. (2017) 45:D362–8. doi: 10.1093/nar/gkw937
23. Niu X, Zhang J, Zhang L, Hou Y, Pu S, Chu A, et al. Weighted gene co-expression network analysis identifies critical genes in the development of heart failure after acute myocardial infarction. *Front Genet*. (2019) 10:1214. doi: 10.3389/fgene.2019.01214
24. Udhaya Kumar S, Thirumal Kumar D, Siva R, George Priya Doss C, Younes S, Younes N, et al. Dysregulation of signaling pathways due to differentially expressed genes from the B-cell transcriptomes of systemic lupus erythematosus patients – a bioinformatics approach. *Front Bioeng Biotechnol*. (2020) 8:276. doi: 10.3389/fbioe.2020.00276
25. Koh GCKW, Porras P, Aranda B, Hermjakob H, Orchard SE. Analyzing protein-protein interaction networks. *J Proteome Res*. (2012) 11:2014–31. doi: 10.1021/pr201211w
26. Gao L, Sun P-G, Song J. Clustering algorithms for detecting functional modules in protein interaction networks. *J Bioinform Comput Biol*. (2009) 07:217–42. doi: 10.1142/S0219720009004023
27. Shih Y-K, Parthasarathy S. Identifying functional modules in interaction networks through overlapping Markov clustering. *Bioinformatics*. (2012) 28:i473–9. doi: 10.1093/bioinformatics/bts370
28. Bernot G, Comet J-P, Richard A, Chaves M, Gouzé J-L, Dayan F. Modeling analysis of gene regulatory networks. In: Cazals F, Kornprobst P, editors. *Modeling in Computational Biology Biomedicine*. Berlin; Heidelberg: Springer (2013). p. 47–80. doi: 10.1007/978-3-642-31208-3_2
29. Dubovenko A, Nikolsky Y, Rakhmatulin E, Nikolskaya T. Functional analysis of OMICS data small molecule compounds in an integrated ‘knowledge-based’ platform. In: Tatarinova TV, Nikolsky Y, editors. *Biological Networks Pathway Analysis Methods in Molecular Biology*. New York, NY: Springer (2017). p. 101–124. doi: 10.1007/978-1-4939-7027-8_6
30. Gao Y, Zhang S, Zhang Y, Qian J. Identification of microRNA-target gene-transcription factor regulatory networks in colorectal adenoma using microarray expression data. *Front Genet*. (2020) 11:463. doi: 10.3389/fgene.2020.00463
31. Bindea G, Mlecnik B, Hackl H, Charoentong P, Tosolini M, Kirilovsky A, et al. ClueGO: a Cytoscape plug-in to decipher functionally grouped gene ontology and pathway annotation networks. *Bioinformatics*. (2009) 25:1091–3. doi: 10.1093/bioinformatics/btp101
32. Zhou Y, Zhou B, Pache L, Chang M, Khodabakhshi AH, Tanaseichuk O, et al. Metascape provides a biologist-oriented resource for the analysis of systems-level datasets. *Nat Commun*. (2019) 10:1523. doi: 10.1038/s41467-019-09234-6
33. Jia Z-Y, Xia Y, Tong D, Yao J, Chen H-Q, Yang J. Module-based functional pathway enrichment analysis of a protein-protein interaction network to study the effects of intestinal microbiota depletion in mice. *Mol Med Rep*. (2014) 9:2205–12. doi: 10.3892/mmr.2014.2137
34. Haider S, Ponnusamy K, Singh RKB, Chakraborti A, Bamezai RNK. Hamiltonian energy as an efficient approach to identify the significant key regulators in biological networks. *PLoS ONE*. (2019) 14:e0221463. doi: 10.1371/journal.pone.0221463
35. Wang X, Yang Q, Liu M, Ma X. Comprehensive influence of topological location and neighbor information on identifying influential nodes in complex networks. *PLoS ONE*. (2021) 16:e0251208. doi: 10.1371/journal.pone.0251208
36. Kim H, Davies P, Walker SI. New scaling relation for information transfer in biological networks. *J R Soc Interface*. (2015) 12:20150944. doi: 10.1098/rsif.2015.0944
37. Li Z, Ren T, Ma X, Liu S, Zhang Y, Zhou T. Identifying influential spreaders by gravity model. *Sci Rep*. (2019) 9:8387. doi: 10.1038/s41598-019-44930-9
38. Jalili M, Gebhardt T, Wolkenhauer O, Salehzadeh-Yazdi A. Unveiling network-based functional features through integration of gene expression into protein networks. *Biochim Biophys Acta BBA Mol Basis Dis*. (2018) 1864:2349–59. doi: 10.1016/j.bbadis.2018.02.010
39. Ozgur A, Vu T, Erkan G, Radev DR. Identifying gene-disease associations using centrality on a literature mined gene-interaction network. *Bioinformatics*. (2008) 24:i277–85. doi: 10.1093/bioinformatics/btn182
40. Bashan A, Bartsch RP, Kantalhardt JW, Havlin S, Ivanov PCH. Network physiology reveals relations between network topology and physiological function. *Nat Commun*. (2012) 3:702. doi: 10.1038/ncomms1705
41. Bindea G, Galon J, Mlecnik B. CluePedia Cytoscape plugin: pathway insights using integrated experimental and *in silico* data. *Bioinformatics*. (2013) 29:661–3. doi: 10.1093/bioinformatics/btt019
42. Bezabih G, Cheng H, Han B, Feng M, Xue Y, Hu H, et al. Phosphoproteome analysis reveals phosphorylation underpinnings in the brains of nurse and forager honeybees (*Apis mellifera*). *Sci Rep*. (2017) 7:1973. doi: 10.1038/s41598-017-02192-3
43. Bohler A, Wu G, Kutmon M, Pradhana LA, Coort SL, Hanspers K, et al. Reactome from a WikiPathways perspective. *PLoS Comput Biol*. (2016) 12:e1004941. doi: 10.1371/journal.pcbi.1004941

44. Meunier D, Lambiotte R, Bullmore ET. Modular and hierarchically modular organization of brain networks. *Front Neurosci.* (2010) 4:200. doi: 10.3389/fnins.2010.00200
45. Finc K, Bonna K, He X, Lydon-Staley DM, Kühn S, Duch W, et al. Dynamic reconfiguration of functional brain networks during working memory training. *Nat Commun.* (2020) 11:2435. doi: 10.1038/s41467-020-15631-z
46. Ali S, Malik MDZ, Singh SS, Chirom K, Ishrat R, Singh RKB. Exploring novel key regulators in breast cancer network. *PLoS ONE.* (2018) 13:e0198525. doi: 10.1371/journal.pone.0198525
47. Mistry D, Wise RP, Dickerson JA. DiffSLC: a graph centrality method to detect essential proteins of a protein-protein interaction network. *PLoS ONE.* (2017) 12:e0187091. doi: 10.1371/journal.pone.0187091
48. Qiao T, Shan W, Zhou C. How to identify the most powerful node in complex networks? A novel entropy centrality approach. *Entropy.* (2017) 19:614. doi: 10.3390/e19110614
49. Singh A, Singh RR, Iyengar SRS. Node-weighted centrality: a new way of centrality hybridization. *Comput Soc Netw.* (2020) 7:6. doi: 10.1186/s40649-020-00081-w

Conflict of Interest: The authors declare that the research was conducted in the absence of any commercial or financial relationships that could be construed as a potential conflict of interest.

The reviewer MA declared a shared affiliation, with six of the authors MA, ST, RA, MS, AA, and RI to the handling editor at the time of the review.

Publisher's Note: All claims expressed in this article are solely those of the authors and do not necessarily represent those of their affiliated organizations, or those of the publisher, the editors and the reviewers. Any product that may be evaluated in this article, or claim that may be made by its manufacturer, is not guaranteed or endorsed by the publisher.

Copyright © 2022 Ahmed, Tazyeen, Haque, Sulimani, Ali, Sajad, Alam, Ali, Bagabir, Bagabir and Ishrat. This is an open-access article distributed under the terms of the Creative Commons Attribution License (CC BY). The use, distribution or reproduction in other forums is permitted, provided the original author(s) and the copyright owner(s) are credited and that the original publication in this journal is cited, in accordance with accepted academic practice. No use, distribution or reproduction is permitted which does not comply with these terms.